Plant Biotechnology Journal
Open Access
aab Association of Applied Biologists
SEB

Plant Biotechnology Journal (2023), pp. 1–15 doi: 10.1111/pbi.14201

The elicitor VP2 from *Verticillium dahliae* triggers defence response in cotton

Ping Qiu[1,2], Baoxin Zheng[1,2], Hang Yuan[1,2], Zhaoguang Yang[1], Keith Lindsey[3], Yan Wang[4], Yuqing Ming[1,2], Lin Zhang[1], Qin Hu[1], Muhammad Shaban[1,5], Jie Kong[6], Xianlong Zhang[1,2] and Longfu Zhu[1,2,*]

[1]*National Key Laboratory of Crop Genetic Improvement, Huazhong Agricultural University, Wuhan, People's Republic of China*
[2]*Hubei Hongshan Laboratory, Huazhong Agricultural University, Wuhan, People's Republic of China*
[3]*Department of Biosciences, Durham University, Durham, UK*
[4]*College of Plant Protection, Nanjing Agricultural University, Nanjing, People's Republic of China*
[5]*Department of Plant Breeding and Genetics, University of Agriculture Faisalabad, Faisalabad, Pakistan*
[6]*Institute of Economic Crops, Xinjiang Academy of Agricultural Sciences, Urumqi, People's Republic of China*

Received 15 June 2023;
revised 25 August 2023;
accepted 29 September 2023.
**Correspondence* (Tel: +86 27 8728 3955; Fax: +86 27 8728 0196; email lfzhu@mail.hzau.edu.cn)

Keywords: cotton, *Verticillium dahliae*, comparative transcriptome analysis, elicitor, induced resistance, germplasm innovation.

Summary

Verticillium dahliae is a widespread and destructive soilborne vascular pathogenic fungus that causes serious diseases in dicot plants. Here, comparative transcriptome analysis showed that the number of genes upregulated in defoliating pathotype V991 was significantly higher than in the non-defoliating pathotype 1cd3-2 during the early response of cotton. Combined with analysis of the secretome during the V991–cotton interaction, an elicitor VP2 was identified, which was highly upregulated at the early stage of V991 invasion, but was barely expressed during the 1cd3-2-cotton interaction. Full-length VP2 could induce cell death in several plant species, and which was dependent on *NbBAK1* but not on *NbSOBIR1* in *N. benthamiana*. Knock-out of VP2 attenuated the pathogenicity of V991. Furthermore, overexpression of VP2 in cotton enhanced resistance to *V. dahliae* without causing abnormal plant growth and development. Several genes involved in JA, SA and lignin synthesis were significantly upregulated in VP2-overexpressing cotton. The contents of JA, SA, and lignin were also significantly higher than in the wild-type control. In summary, the identified elicitor VP2, recognized by the receptor in the plant membrane, triggers the cotton immune response and enhances disease resistance.

Introduction

The coevolutionary arms race between plants and pathogens has led to the formation of complex pathogenic and defensive mechanisms (Zhou and Zhang, 2020). Fungal pathogens usually deliver various effector proteins into the plants that disrupt intrinsic immunity and help pathogens to colonize successfully (Okmen *et al.*, 2022; Wang *et al.*, 2022a). For example, fungal CFEM effectors of *F. graminearum* interact with ZmLRR5 and ZmWAK17ET to compromise ZmWAK17-mediated resistance (Zuo *et al.*, 2022). The secreted protein VdSCP41 can interact with the plant transcription factors CBP60g and SARD1, inhibiting the transcription of CBP60g, thus inhibiting the induction of plant immune related genes, and promoting infection by *V. dahliae* (Qin *et al.*, 2018). For necrotrophic pathogens, the successfully invading pathogens will secrete a large number of proteins that promote the hypersensitive response (HR) and cell death and obtain nutrients for colonization and reproduction (Bi *et al.*, 2023; Tian *et al.*, 2020). For example, the necrotrophic fungal pathogen *Parastagonospora nodorum* employs necrotrophic effectors (NEs) to induce tissue necrosis on wheat leaves during infection and lead to septoria nodorum blotch (SNB) (John *et al.*, 2022).

In response to attack by pathogens, plants have evolved two categories of immune systems to recognize pathogens and activate specific defence responses (Wang *et al.*, 2020; Zhou and Zhang, 2020). Pattern recognition receptors (PRRs) located on plant cytoplasmic membranes can recognize pathogen-associated molecular patterns (PAMPs) or microbial associated molecular patterns (MAMPs) to trigger defence responses (namely PAMP triggered immunity, PTI), which is the first category (Escocard de Azevedo Manhães *et al.*, 2021; Jones and Dangl, 2006). PRRs typically interact with coreceptors to activate downstream immune responses (Ngou *et al.*, 2021). For instance, flagellin-sensitive 2 (FLS2) and BAK1 (BRI1-associated receptor kinase 1) form a complex to initiate plant defence (Chinchilla *et al.*, 2007). The kinase AtLYK5 forms a chitin-induced complex with related kinase AtCERK1 to induce plant immunity in Arabidopsis (Cao *et al.*, 2014). These coreceptors are highly conserved in plants and are crucial for PRR-mediated immunity. Plants can also use intracellular or transmembrane receptors to recognize specific effector proteins secreted by pathogens and trigger stronger immune responses, called effector activated immunity (ETI), which belongs to the second category (Jones and Dangl, 2006; Zhou and Zhang, 2020). Many proteins and peptide elicitors that could induce plant defence responses have been discovered (Pemberton and Salmond, 2004; Sun *et al.*, 2013). For instance, the N-terminus 22 amino acid peptide of glycosyl-phosphatidyl-inositol-anchored protein (SGP1) from *Ustilaginoidea virens* can elicit cell death, oxidative burst, and defence-related gene expression (Song *et al.*, 2021). An

Please cite this article as: Qiu, P., Zheng, B., Yuan, H., Yang, Z., Lindsey, K., Wang, Y., Ming, Y., Zhang, L., Hu, Q., Shaban, M., Kong, J., Zhang, X. and Zhu, L. (2023) The elicitor VP2 from *Verticillium dahliae* triggers defence response in cotton. *Plant Biotechnol. J.*, https://doi.org/10.1111/pbi.14201.

elicitor PevD1 secreted by *V. dahliae* can induce multiple defence responses in plants (Liang *et al*., 2021). PTI and ETI immune systems are not independent of each other, but reinforce each other, which leads to a stronger calcium ion influx, more ROS accumulation, and callose deposition (Ngou *et al*., 2021; Yuan *et al*., 2021).

Verticillium dahliae (*V. dahliae*) is a typical soil-borne vascular pathogenic fungus that causes disease in more than 200 species of dicotyledonous plants (Fradin and Thomma, 2006). Infected plants usually exhibit leaf wilting, yellowing, necrosis, or even plant death (Jiménez-Díaz *et al*., 2011). In the process of coevolution with the host, due to the influence of heterokaryosis and ecological environment differences, *V. dahliae* often produces physiological differentiation and new pathogenic isolates, and rapidly emerging new strains can inactivate the corresponding resistance genes in the host and promote susceptibility (Inderbitzin and Subbarao, 2014). The lack of disease-resistant cotton germplasm and the variation across pathogen isolates have led to the urgent problems in cotton production (Xu *et al*., 2011). Studies have shown that many elicitors from pathogens can improve plant disease resistance (Li *et al*., 2022; Sands *et al*., 2022). For instance, multiple harpins expressed in wheat, cotton, and soybean showed enhanced plant resistance to pathogens (Du *et al*., 2018; Fu *et al*., 2014; Miao *et al*., 2010). Aspf2-like protein VDAL, secreted by *V. dahliae*, causes leaf wilting *in vitro*, but when overexpressed in Arabidopsis or cotton, promotes resistance to *V. dahliae* without affecting plant growth and development (Ma *et al*., 2021). Consequently, the identification of elicitors that can induce plant immune activation might be used to enhance plant disease resistance.

In this study, a secretory protein elicitor VP2 from *V. dahliae* was identified through comparative transcriptome and secretome analysis. VP2 can trigger HR and cell death in *N. benthamiana*, Arabidopsis, and cotton. VP2 was overexpressed in transgenic cotton plants and thoroughly investigated for response to infection by *V. dahliae*. The obtained results provide new insights in disease resistance mechanisms and breeding in cotton.

Results

Comparative transcriptome analysis of *V. dahliae*-cotton interaction

In order to compare the interaction differences between *V. dahliae* isolates in the early infection response of cotton, the defoliating isolate V991 and non-defoliating isolate 1cd3-2 were each co-cultured with roots from *G. barbadense* cv. 7124 and *G. hirsutum* cv. YZ1 for 3 days, respectively, filtered and collected by centrifugation for transcriptome sequencing (Figure 1a). The differentially expressed genes (DEGs) showed similar transcriptional patterns in the same strain, which also implied that the experiment had good repeatability (Figure 1b,c). The expression profile showed that most of DEGs of 1cd3-2 were downregulated (Figure 1b,d), and the number of upregulated DEGs of V991 was significantly higher than for 1cd3-2 (Figure 1d).

There were 2063 shared DEGs among the four transcriptomes, which may be conserved in the interaction between the host and *V. dahliae* (Figure 1e). GO enrichment analysis shows that they were mainly associated with DNA metabolic process, histone methylation, transmembrane transport, transcription, DNA-templated, organonitrogen compound catabolic process, cellular response to stress, and cell division (Figure 1f). More DEGs were found during the interactions with different isolates. In total, 1601 DEGs were specific to the interaction between 1cd3-2 and cotton (Figure 1e) and were mainly enriched in vesicle docking involved in exocytosis, cell communication, cellular protein modification process, secretion by cell, signal transduction, growth, lipid translocation, and filamentous growth through GO enrichment analysis (Figure 1g). In total, 2493 DEGs were specific to the interaction between V991 and cotton (Figure 1e) and were mainly enriched in glycolytic process, carbohydrate derivative metabolic process, carbohydrate metabolic process, cellular response to oxidative stress, positive regulation of hydrolase activity, small molecule metabolic process, and cell wall modification (Figure 1h). All these data indicated that the more aggressive defoliating isolate V991 activated more signalling and metabolic pathways during the pathogen–host interaction.

Screening of V991 key candidate secretory proteins

Label-free-based secretome was used to identify the key candidate secretory proteins produced by V991, and PCA showed good intragroup repeatability (Figure S1a). A total of 790 proteins were identified in the secretome (Figure S1b). Among them, 111 proteins were specifically identified in the treatment group and 23 proteins in the control group (Figure S1b; Table S4); There were 656 proteins that were found in both groups, of which 174 were upregulated proteins and 64 were downregulated in the treatment group (Figure S1b; Table S3). In total, 268 genes accounting for 34% were predicted to encode secreted proteins (possessing the extracellular localization signal peptide (SP) and lack a transmembrane motif). Of these, 168 were less than 500 amino acids in size and rich in cysteines (cysteine number ≥ 2)

Figure 1 Comparative transcriptome analysis of the interaction between *V. dahliae* and cotton. (a) The sampling mode diagram of transcriptomes. V991 and 1cd3-2 were each co-cultured with roots from *G. barbadense* cv. 7124 (Hai7124) and *G. hirsutum* cv. YZ1 (YZ1) for 3 days, respectively, filtered and collected by centrifugation for transcriptome sequencing. The spores of the two pathogens cultured in liquid medium (Czapek-Dox) without roots for 3 days were used as the control, respectively. (b) Expression profiles of differentially expressed genes (DEGs) involved in the interaction of 1cd3-2 with different cotton roots. The gene expression values were calculated using the FPKM method. The scale bar represents expression value of each gene after row normalization by removing the mean and dividing by the standard deviation. Upregulated and downregulated genes are shown in red and blue colours, respectively. (c) Expression profiles of DEGs involved in the interaction of V991 with different cotton roots. (d) The number of DEGs in V991 and 1cd3-2 transcriptomes, respectively. Statistical analyses were performed using a Student's *t* test: ns, Not significant; $*P < 0.05$. (e) Venn diagram showing the number of DEGs in different transcriptomes. 1cd3-2-H3 and 1cd3-2-Y3 represent the transcriptomes of 1cd3-2 interacting with roots from Hai7124 and YZ1 3 days post inoculation (dpi), respectively. V991-H3 and V991-Y3 represent the transcriptomes of V991 interacting with roots from Hai7124 and YZ1 3 dpi, respectively. (f) GO enrichment analysis of 2063 DEGs shared in the four transcriptomes. Gene ratio is the number of DEGs divided by the total number of genes associated with a specific pathway. (g) GO enrichment analysis of 1601 DEGs shared in 1cd3-2 transcriptome only. (h) GO enrichment analysis of 2493 DEGs shared in the V991 transcriptome only.

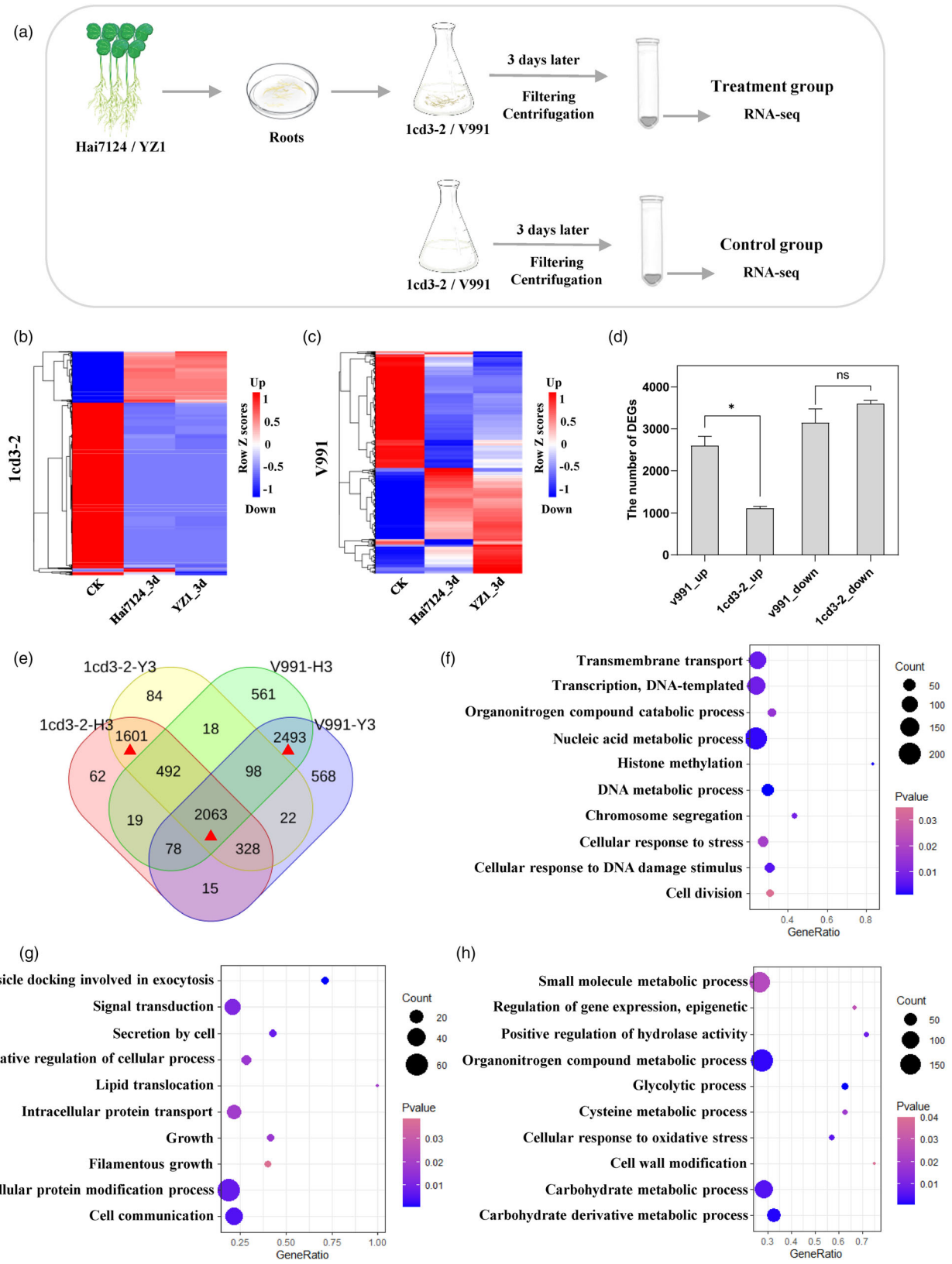

(Figure S1c,d). Finally, 10 cysteine-rich secretory proteins (VPs) were identified as having high transcript levels during the interaction between V991 and cotton (Table S1; Figure S2).

VP2 triggers cell death in plants

To verify whether VPs can act as elicitors to trigger plant defence responses, VPs were cloned into the overexpression vector fused with the GFP tag, and *N. benthamiana* leaves were injected with *Agrobacterium* containing the constructs to monitor the effects of transient expression. Only VP2 was found to trigger the HR and cell death in *N. benthamiana* (Figure 2a). VP2 lacking the signal peptide ($VP2^{-SP}$) was unable to trigger necrosis in *N. benthamiana* leaves (Figure 2a). Western blot analysis confirmed the expression of VP2 and $VP2^{-SP}$ (Figure 2b). Full-length VP2 also induced cell death in leaves of Arabidopsis, which was not observed for GFP control (Figure 2c). Cotton leaves showed obvious necrosis 4 days later upon infiltration of VP2-GST recombinant protein supernatant (from *Escherichia coli*) (Figure 2d,e). However, $VP2^{-SP}$-GST recombinant protein supernatant did not cause cell death in cotton leaves (Figure 2d,e). The expression of genes related to HR and PAMP-responsive was determined in *N. benthamiana*. The results showed that VP2 could significantly activate the expression of genes involved in HR, like *HSR203* and *HIN1*, and PTI-related genes, like *NbAcre31*, *Nbpia5*, *NbCYP71D20*, and *NbWRKY7* (Figure 2f). These suggested that VP2 acts as an elicitor that can be recognized by multiple plant species and trigger the immune response.

NbBAK1 but not *NbSOBIR1* is required for VP2-induced cell death

Subcellular localization experiments demonstrated that VP2 was localized to the *N. benthamiana* plasma membrane (Figure 3a), while $VP2^{-SP}$ localized in both plasma membrane and nucleus (Figure 3a). This suggested that plant cell death triggered by VP2 depends on the membrane localization. Virus-induced gene silencing (VIGS) was employed to silence *NbBAK1* and *NbSOBIR1* in *N. benthamiana* (Figure 3b), and qRT-PCR analysis confirmed that the expression of *NbBAK1* or *NbSOBIR1* was markedly knocked down (Figure 3c). The results showed that VP2 did not induce cell death in *NbBAK1*-silenced *N. benthamiana* leaves, but strongly triggered cell death in *NbSOBIR1*-silenced leaves, similar to the results from *GFP*-silenced *N. benthamiana* leaves (Figure 3b). Immunoblotting analysis confirmed that VP2 was successfully expressed in the *NbBAK1* or *NbSOBIR1*-silenced plants (Figure 3d). These results suggested that *NbBAK1* but not *NbSOBIR1* are required for VP2-induced cell death.

VP2 contributes to the virulence of *V. dahliae*

BLAST analysis revealed that VP2 was only found in *Verticillium* spp., though with no known function (Table S1). The amino acid sequence of VP2 in V991 and 1cd3-2 is very conserved, and only two amino acids are variant in the signal peptide region (Figure S3). A yeast capture system showed that the signal peptide of both genotypes has secretory function (Figure S4). To further detect the expression levels of VP2, total RNA was extracted from infected cotton hypocotyls at 6, 18 days post inoculation (dpi). qRT-PCR results showed that VP2 in defoliating isolates V991 and T9 was highly expressed at 6 dpi, while the transcript of VP2 in non-defoliating isolates 1cd3-2 and BP2 was very low during the invasion process (Figure 4a). These results implied that the expression of VP2 might be regulated specifically by the defoliating pathotype of *V. dahliae* in the early stage of invasion.

To further investigate VP2 function in fungal virulence, two independent knockout mutants *ΔVP2* (*ΔVP2-1*, *ΔVP2-2*) and two ΔVP2/VP2-complementation transformants (Com-1, Com-2) were obtained for V991 (Figure S5). The growth rate and mycelium morphology of the VP2 knockout mutants were similar to the WT (V991) and complementation transformants (Figure S5b,c), while knock-out of VP2 significantly reduced the virulence of the pathogen, with less chlorotic leaf formation and disease index compared to the wild type and complementation transformants (Figure 4b,c).

Heterologous expression of VP2 enhances cotton resistance to *V. dahliae*

Since VP2 acts as an elicitor that can cause rapid necrosis of cotton cotyledons (Figure 2d), *VP2*-overexpressing cotton lines were generated to investigate the regulatory mechanism (Figure 5a,b). qRT-PCR results showed that the transcription levels of VP2 were high in roots and leaves of the cotton lines *OEVP2-1*, *OEVP2-2*, and *OEVP2-3* (Figure 5a). VP2 protein was also detected in transgenic lines by immunoblotting (Figure 5b). The transgenic cotton did not show any growth or developmental defects comparable to wild-type controls in the greenhouse (Figure 5c). However, after inoculation with *V. dahliae*, transgenic plants exhibited enhanced resistance, with mild symptoms and a lower disease index (Figure 5d,g). Consistent with this, less browning of vascular tissue (Figure 5e) and the fungal recovery assay (Figure 5f) all supported the view that VP2 enhanced cotton resistance to *V. dahliae*. Similarly, in the field, VP2 transgenic plants also showed significantly improved their tolerance to Verticillium wilt (Figure S6).

VP2 triggers the cotton immune system and defence response

Transcriptome analysis of uninoculated transgenic plants showed that 805 genes were DEGs compared to the wild type, of which 314 DEGs were up-regulated and 491 DEGs were down-regulated. GO enrichment analysis showed that DEGs were significantly enriched in response to stress, defence response, cell wall modification, and systemic acquired resistance and lignin metabolic process (Figure 6a). Among these, 15 genes that suggested to

Figure 2 VP2 full-length induced multiple plants cell death and stimulate immune response. (a) Transient expression of VP2 and $VP2^{-SP}$ in *N. benthamiana* leaves. (b) Immunoblotting analysis of transiently expressed VP2 and $VP2^{-SP}$ fused to the GFP tag in *N. benthamiana* leaves 48 h after infiltration. (c) Transient expression of VP2 in Arabidopsis through agroinfiltration. (d) The protein supernatant of VP2 prokaryotic expression causes cotton cotyledons wilt. Photos were taken on day 4. The plants were kept at 25 °C with 70% relative humidity. (e) Immunoblotting analysis of prokaryotic expression protein VP2 and $VP2^{-SP}$ fused to the GST tag. (f) qRT-PCR of marker genes related to hypersensitivity response (HR) and PAMP responsive in *N. benthamiana* leaves. Leaves were sampled for RNA extraction at 2 days after agro-infiltration of VP2, GFP, and INF1. GFP and INF1 were used as the negative control and positive control, respectively. Transcript levels of genes were normalized to the levels of the constitutive reference gene *NbEF1a*. The values are means ± SD, $n = 3$, and the values in GFP were normalized as 1. Statistical analyses were performed using a Student's *t* test: $*P < 0.05$; $**P < 0.01$; $***P < 0.001$.

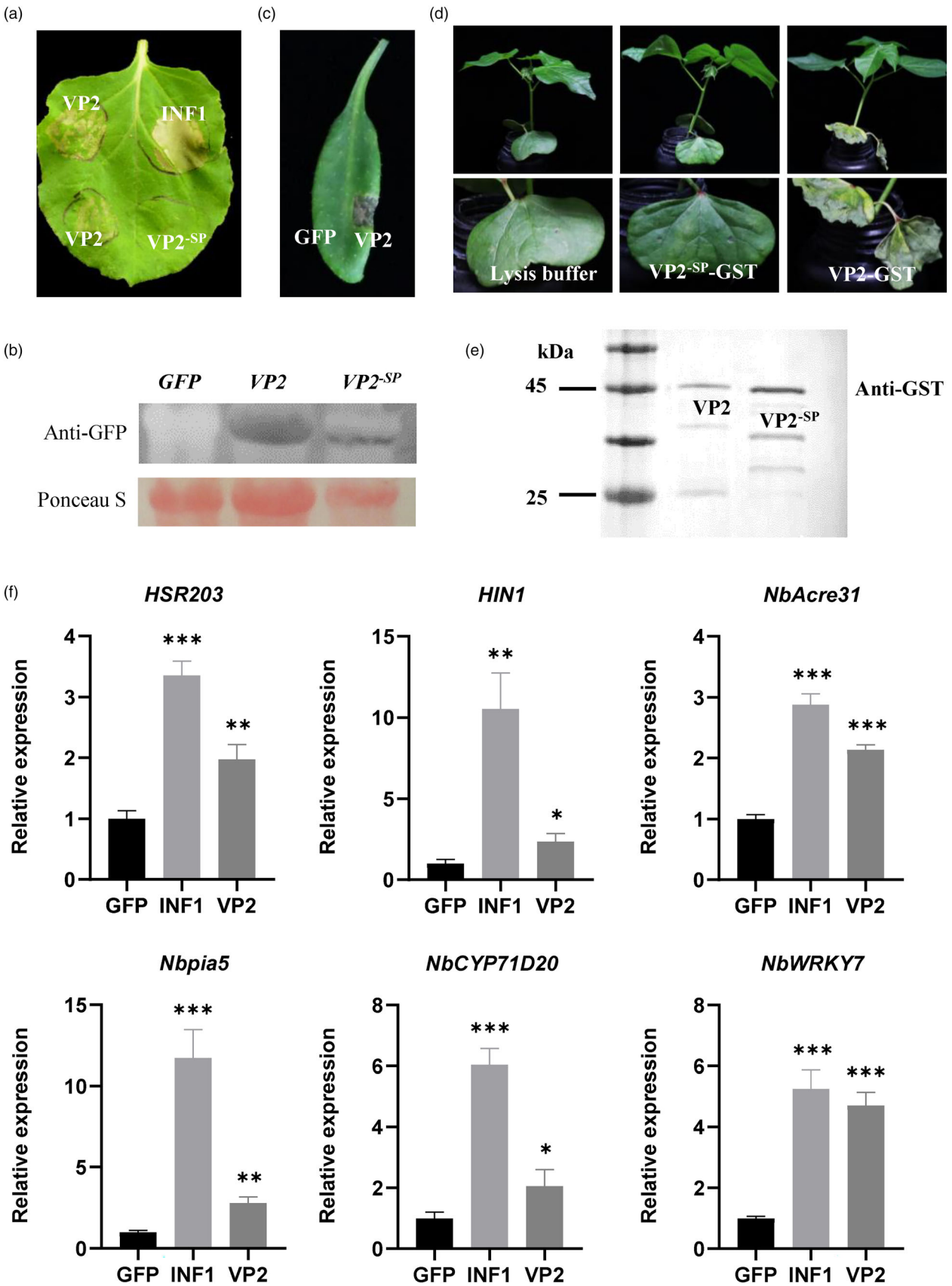

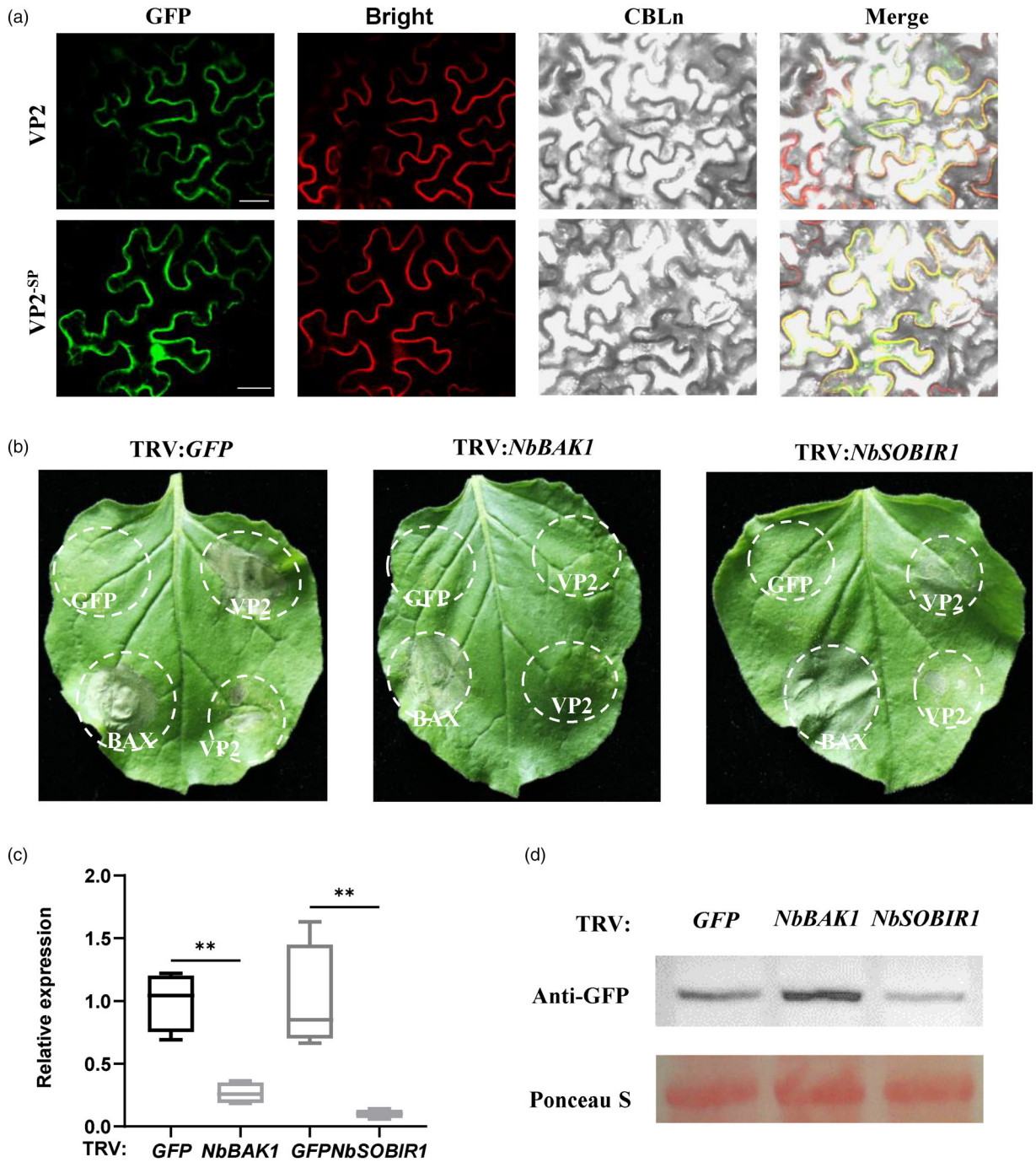

Figure 3 *NbBAK1* but not *NbSOBIR1* is required for VP2-induced cell death. (a) Analysis of green fluorescent protein (GFP) in *N.benthamiana* epidermal cells expressing 35S::VP2:GFP, 35S::VP2^{-SP}:GFP and red fluorescent protein (CBLn) expression in *N. benthamiana* through agroinfiltration. CBLn localizes in the plant cell membrane used as a positive control in localization studies. Fluorescence from epidermal cells in the infiltrated tissues was detected by confocal microscopy at 48 h post agroinfiltration. Scale bars, 30 μm. (b) Virus-induced gene silencing (VIGS) technology was used to silence *NbBAK1* and *NbSOBIR1* by inoculation with TRV constructs (pTRV2-*GFP*, pTRV2-*NbBAK1*, and pTRV2-*NbSOBIR1*) in *N. benthamiana* leaves. Three weeks after inoculation, GFP, BAX, VP2 were transiently expressed in *NbBAK1*-and *NbSOBIR1*-silenced *N. benthamiana* plant leaves. Photographs were taken 3 days after agroinfiltration. The experiment was carried out three times with five plants for each TRV construct. (c) The expression levels of *NbBAK1* and *NbSOBIR1* after VIGS treatment as evaluated by qRT-PCR. *NbEF1a* was used as the internal reference gene. Statistical analyses were performed using a Student's *t* test: $^{**}P < 0.01$. (d) Immunoblotting analysis of transiently expressed VP2 in *NbBAK1*- and *NbSOBIR1*-silenced *N. benthamiana* leaves.

participate in the plant immune response were identified (Figure 6b). The expression level of these genes was higher in *VP2*-overexpressing cotton lines compared with the wild type under normal growth conditions, and they were induced more quickly and to higher levels upon inoculation with V991 in the over-expressers (Figure 6b). Further experiments showed that the expression levels of genes involved in the SA signalling pathway, including *GhPR1*, *GhPR2*, and *GhPR5* and JA signalling-related

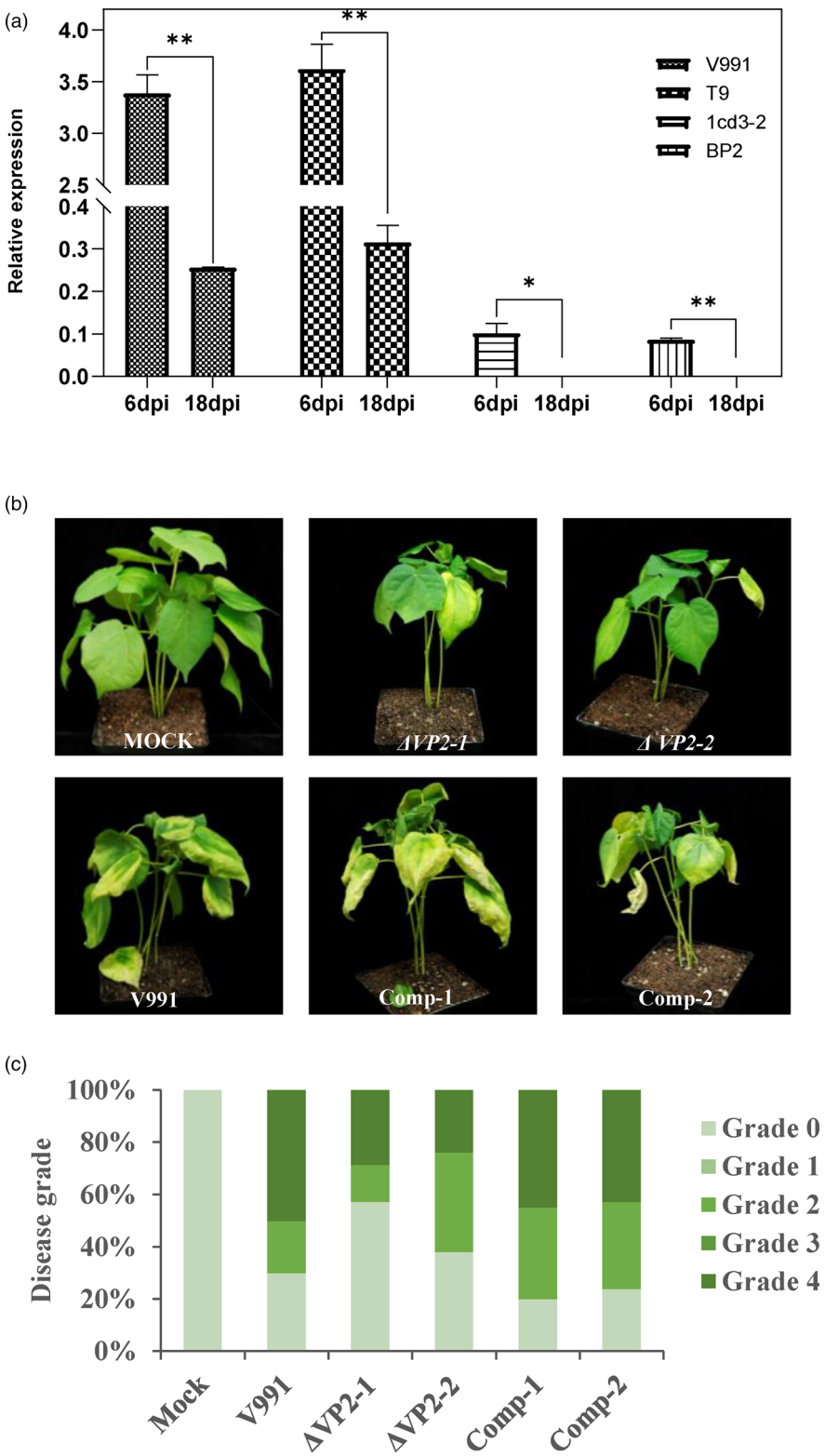

Figure 4 VP2 is essential for the full virulence function of *V. dahliae*. (a) Expression of VP2 in defoliating pathotype and non-defoliating pathotype *V. dahliae* at 6, 18 dpi, respectively. The *v991_EVM0005718* was used as the internal control gene. The values are means ± SD, $n = 3$. Statistical analyses were performed using a Student's *t* test: $*P < 0.05$; $**P < 0.01$. (b) Infection assays of wild-type V991, *ΔVP2* mutants, and *ΔVP2*/VP2-complementation transformants on cotton. Three-week-old cotton seedlings were inoculated with 10^6 mL^{-1} of conidia from V991, *ΔVP2-1*, and *ΔVP2-2* strains, and complementary transformants Comp-1 and Comp-2. Photographs were taken at 16 dpi. (c) Disease index of infected cotton plants. The disease grade was classified as follows: 0 (no symptoms), 1 (0%–25% wilted leaves), 2 (25%–50% wilted leaves), 3 (50%–75% wilted leaves), and 4 (75%–100% wilted leaves). The grades of disease symptoms were calculated with three replicates of 30 plants.

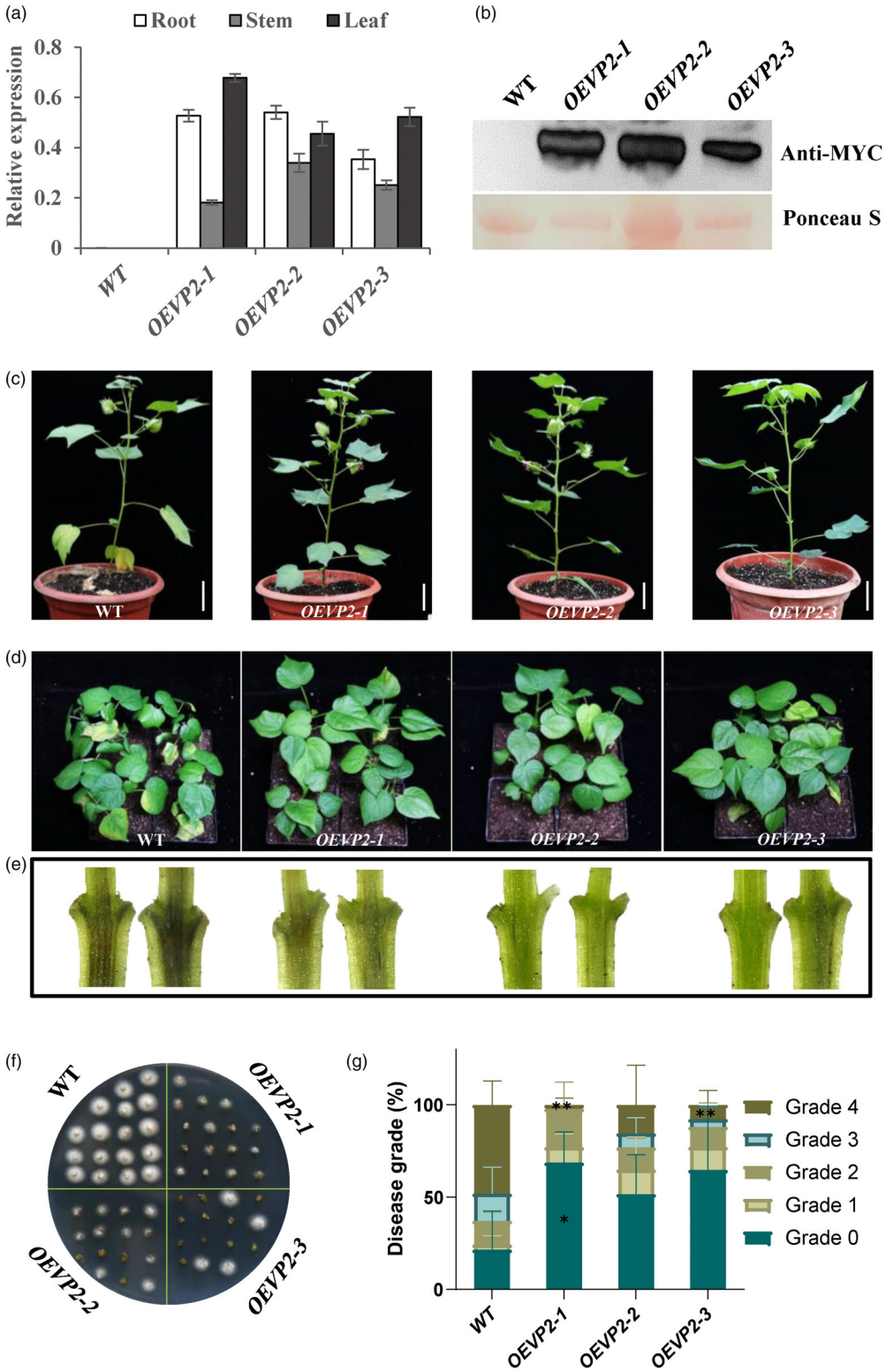

Figure 5 Cotton expressing VP2 are resistant to infection by *V. dahliae*. (a) and (b) The molecular evidence of transgenic cotton. (a) Analysis of the tissue expression pattern of VP2 in transgenic cotton lines. The *GhUB7* was used as the internal control gene. The data were generated from three replicates of experiments. (b) Immunoblot analysis of VP2 in three transgenic cotton lines overexpressing VP2. Total proteins of 18-day-old seedlings were extracted and detected with anti-MYC antibodies. (c) The growth phenotype of transgenic lines in greenhouse. Scale bars, 6 cm. (d) Disease symptoms of WT and *OEVP2* plants infected by *V. dahliae* and photographed at 16dpi. (e) Comparison of sections from cotyledonary node between WT and *OEVP2* plants at 18 dpi; (f) fungal recovery assay of cotyledonary node sections from WT and *OEVP2* plants at 18 dpi and photographed 7 days after culturing. (g) The statistics of disease grade after inoculation with V991 for 16 dpi. The values are means ± SD, $n = 3$. Statistical analyses were performed using a Student's *t* test: $^{*}P < 0.05$; $^{**}P < 0.01$.

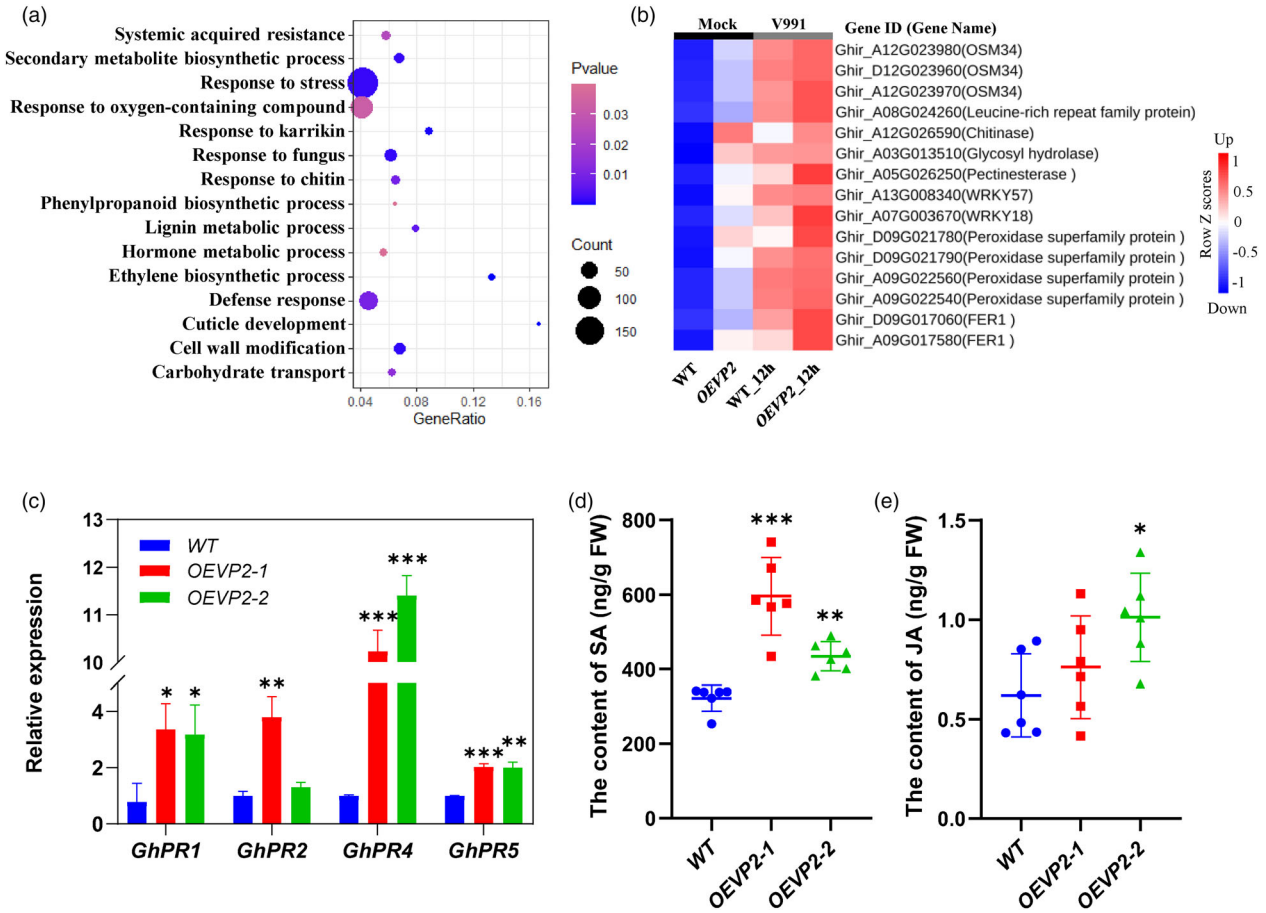

Figure 6 The content of SA and JA increased in VP2 transgenic cotton. (a) Gene ontology enrichment of DEGs from *OEVP2 versus* WT. Gene ratio is the number of DEGs divided by the total number of genes associated with a specific pathway. (b) Heat map of the expression of genes associated with disease resistance in the transcriptomes. The gene expression value was calculated using the FPKM method. The scale bar represents expression value of each gene after row normalization by removing the mean and dividing by the standard deviation. Upregulated and downregulated genes are shown in red and blue, respectively. (c) qRT-PCR analysis of SA (*PR1*, *PR2*, and *PR5*) and JA (*PR4*) biosynthesis and signalling genes in WT and *OEVP2* plants under normal growth conditions. The values represent means ± SD, $n = 3$. *GhUB7* was used as the internal control gene. All values in WT were normalized as 1. Statistical analyses were performed using a Student's *t* test: *$P < 0.05$; **$P < 0.01$; ***$P < 0.001$. (d) and (e) Measurement of SA (d) and JA (e) content in WT and *OEVP2* cotton plants under normal growth conditions. The values represent means ± SD, $n = 6$. Statistical analyses were performed using a Student's *t* test: *$P < 0.05$; **$P < 0.01$; ***$P < 0.001$.

GhPR4, were significantly higher in *VP2*-overexpressing cotton lines than in the WT under normal growth conditions (Figure 6c). The SA and JA contents were also higher in *VP2*-overexpression lines (Figure 6d,e).

More genes involved in cell wall modification and lignin metabolism were identified and analysed in the *VP2*-overexpression lines through transcriptome analysis (Figure 6a). Expression pattern analysis confirmed that *GhPALs* were significantly more highly expressed in *VP2*-overexpressing cotton than in the WT, regardless of whether inoculated with pathogen or not (Figure 7a,b). In addition to *GhPALs*, other lignin synthesis related genes such as *GhCCoAOMT*, *GhF5H-6*, *GhF5H-7*, and *Gh4CL-1* were also higher in *VP2*-overexpressing cotton lines under normal growth conditions (Figure S7). Phloroglucinol-HCl staining of stem cross-sections showed that lignin deposition was clearly increased in *VP2*-overexpressing cotton compared with the WT (Figure 7c). Lignin content assays were consistent with the histochemical staining, showing significantly increased accumulation in *VP2*-overexpressing lines than in the wild-type control (Figure 7d). All these data suggested that VP2 triggers the cotton immune system by activating phytohormone synthesis and phenolic metabolite biosynthesis.

Discussion

Defoliating *V. dahliae* regulates the upregulation of more DEGs

The coevolution between host plants and their pathogens is a dynamic process (Woolhouse *et al.*, 2002). This competitive evolution drives frequent changes in the gene sequence and promoter, such as single-nucleotide polymorphisms (SNPs), insertion, and deletion, making these genes highly polymorphic (Guttman *et al.*, 2014; Wang *et al.*, 2022b). For example, the serine substitution of glycine in Phytophthora avirulence effector PsAvr3c leads to evasion of Rps3c-mediated soybean immunity (Huang *et al.*, 2018). The secreted protein Ps109281 of *Phytophthora sojae*, due to its N-terminal sequence polymorphism, cannot trigger plant cell death like other GH12 members

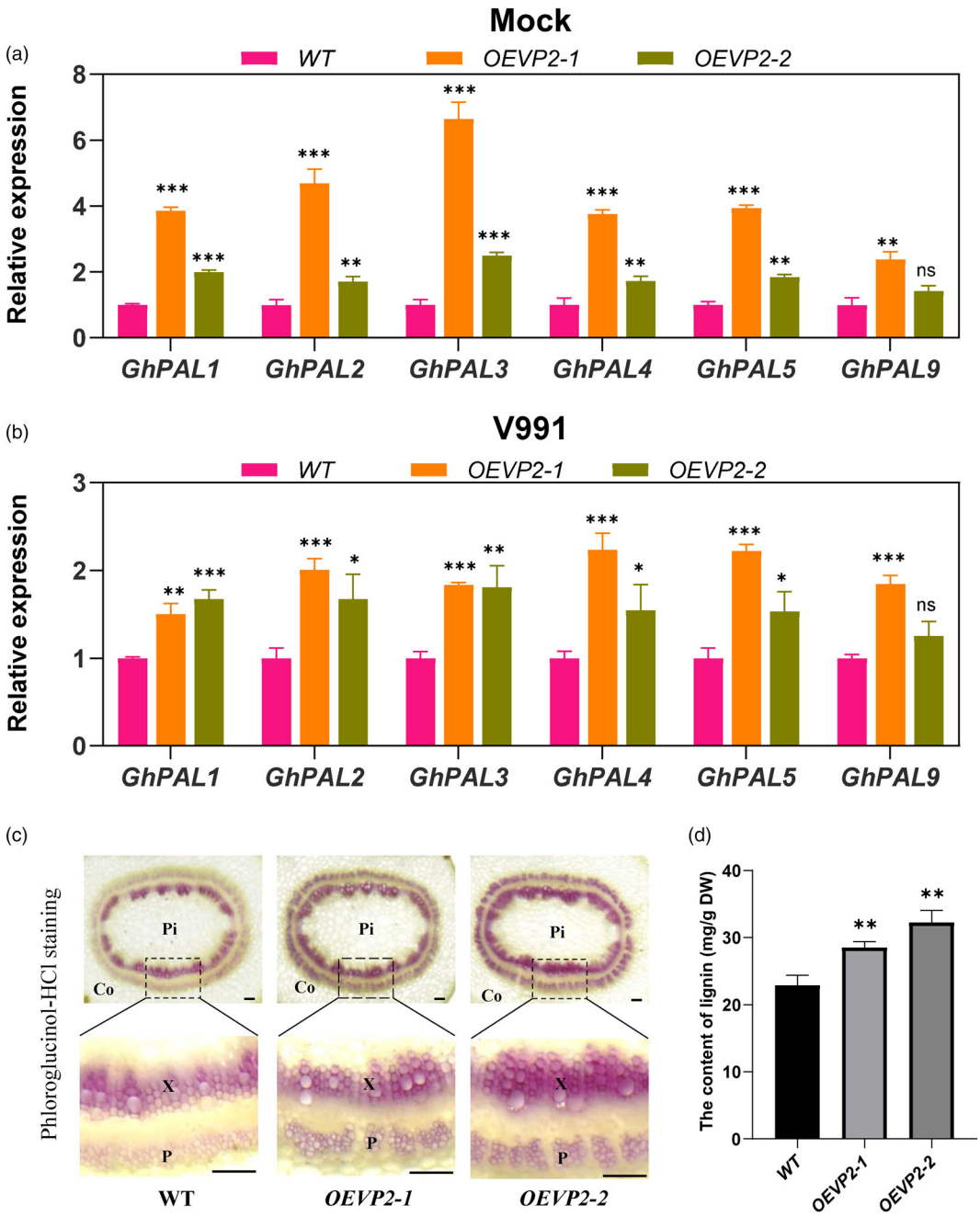

Figure 7 Overexpression of VP2 in cotton promotes lignin accumulation. (a) and (b) qRT-PCR analysis of *GhPALs* in WT and *OEVP2* transgenic cotton lines without (a)/with (b) inoculation for 12 h. The values are means ± SD, $n = 3$, and normalized with *GhUB7*, and then all values in WT were normalized as 1. Statistical analyses were performed using a Student's *t* test: ns, Not significant; *$P < 0.05$; **$P < 0.01$; ***$P < 0.001$. (c) The histochemical analysis to observe the lignin deposition in stem from WT and *OEVP2* transgenic cotton lines under normal growth conditions. Co: cortex, P: phloem, X: xylem, Pi: pith. The scale bar stands for 100 μm. (d) The determination of the lignin in the WT and *OEVP2* transgenic cotton lines under normal growth conditions. The values represent the means ± SD; $n = 3$. Student's *t* test: **, $P < 0.01$.

(Wang *et al*., 2022b). In addition, the resistance-breaking isolates carrying unexpressed alleles evades being recognized by RPP4-containing Arabidopsis (Asai *et al*., 2018). Recently, a natural variation in the hrpL promoter was found and made *Pseudomonas syringae* loss its virulence (Xie *et al*., 2023). To understand the virulence mechanisms of *V. dahliae*, most studies have focused on differences at the genomic level (Chen *et al*., 2018; Jonge *et al*., 2013). Here, our results show that defoliating isolate V991 might enhance its virulence by increasing the expression of more virulence-related genes during invasion of the host compared with 1cd3-2. Defoliating isolate V991 regulates more DEGs upregulated expression, and V991-specific DEGs are significantly enriched in the processes of hydrolase activity, small molecule metabolism, carbohydrate metabolism, and cell wall modification (Figure 1). Previous studies also showed that carbohydrate hydrolases (CAZymes) play an important role in promoting pathogen infection and virulence (Ma *et al*., 2015; Wang *et al*., 2021; Zhang *et al*., 2021). These results further indicated

that the genes from defoliating isolates of *V. dahliae* that specifically respond to the host may play an important role in the virulence differentiation of *V. dahliae*.

In this study, a key virulence factor VP2 was identified, which has only two amino acid variations in the signal peptide region between the defoliating and non-defoliating pathotype *V. dahliae*, and does not affect its secretory function. However, compared to D-type VP2 being induced at the early stage of invasion, ND-type VP2 was almost not induced during the invasion of the host, which also suggested that different expression of *VP2* may influence the virulence of *V. dahliae*. Studies have shown that cis- and trans-regulatory changes are the main causes of gene differential expression (Wittkopp *et al*., 2004). Among them, transcription factors (TFs) have been extensive studied and are considered important for gene expression (Lai *et al*., 2022; Xiao *et al*., 2021). Therefore, identifying key regulators that regulate the expression of virulence-related downstream genes in *V. dahliae* may play an important role in further elucidating the virulence differentiation of *V. dahliae* isolates.

Improving plant resistance by utilizing pathogenic elicitors

Over the past decades, research has uncovered a multitude of effectors from pathogens and revealed their ability to enhance plant disease resistance (Li *et al*., 2022; Sands *et al*., 2022; Yu *et al*., 2020). For instance, the class II hydrophobin Hyd1 from *Trichoderma harzianum* can induce maize resistance against *C. lunata* (Yu *et al*., 2020). Overexpression of Ave1 in *Ve1* tomato induces the expression of defence genes (Castroverde *et al*., 2016). In this study, we found that VP2, as an elicitor, can cause the necrosis of *N. benthamiana*, Arabidopsis, and cotton leaves and activate plant immunity (Figure 2). Subcellular localization demonstrated that VP2 was located in the plasma membrane (Figure 3). These data suggested that VP2 may act as an PAMP molecule that can be recognized by multiple plant species. Previous studies reported that the receptor-like kinases *BAK1* and *SOBIR1* are required in various PAMP-triggered immune responses (Ma *et al*., 2015; Sun *et al*., 2013; Wang *et al*., 2021; Zhang *et al*., 2023). Receptor-like related kinase *BAK1* can interact with a variety of defence-related proteins and plays an important role in plant immunity (Chinchilla *et al*., 2009). For example, a *N. benthamiana* elicitin-insensitive RLK1 (NbEIR1) regulates *Phytophthora* resistance by coupling with BAK1 to enhance elicitin-triggered immunity (Zhang *et al*., 2023). The *Pseudomonas* effector HopB1 can specifically degrade BAK1, thereby increasing its virulence without overly perturbing the host plant (Li *et al*., 2016). In this study, VIGS experiments in *N. benthamiana* showed that VP2-induced cell death depended on *NbBAK1* rather than *NbSOBIR1* (Figure 3). However, whether VP2 interacts with BAK1 in cotton needs further study.

Plants are constantly attacked by various pathogens and pests, causing massive yield and quality losses annually (Zhou and Zhang, 2020). An effective approach to enhance resistance to diseases is to enhance the immune system of plants through genetic engineering technology (He *et al*., 2023). For example, overexpression of the laccase gene *GhLac1* in cotton can lead to increased lignification and confer an enhanced defence response to both pathogens and pests (Hu *et al*., 2018). uORFsTBF1-mediated NPR1 translation control enhances rice disease resistance without compromising plant fitness (Xu *et al*., 2017). The use of pathogen elicitors that can induce plant immunity is also an effective approach to innovate plant disease resistant germplasm (Ma *et al*., 2021; Rajput *et al*., 2015). In this study, VP2 can induce HR and necrosis in multiple plant species, indicating that there is a conserved mechanism for recognizing VP2 and inducing immune activation, and heterologous overexpression of *VP2* in cotton can significantly increase resistance to *V. dahliae*. The RNA-seq data showed direct evidence for the activation of plant immune-related gene expression by VP2 and during VP2-mediated plant immunity.

Although in most cases, SA and JA have antagonistic relationship, studies have also shown that SA and JA signalling pathways may be necessary together in plant defence responses (Nomoto *et al*., 2021; van Wees *et al*., 2000; Zhu *et al*., 2021). For example, Simultaneous activation of SA- and JA-dependent defence pathways can enhance the induced disease resistance in *Arabidopsis thaliana* (van Wees *et al*., 2000; Xiang *et al*., 2011). In rice, OsWRKY45-1-regulated Xanthomonas oryzae pv oryzae (Xoo) resistance was accompanied by increased accumulation of SA and JA (Tao *et al*., 2009). And knockdown of GhRPS6 results in the reduction of SA and JA content, enhancing cotton more susceptible to *V. dahliae* (Zhu *et al*., 2021). For hemi-biotrophic pathogens such as *V. dahliae*, simultaneously activating SA and JA in plants may be more beneficial for enhancing their resistance to pathogens (Glazebrook *et al*., 2003; Li *et al*., 2023). In our study, VP2 transgenic plants showed significantly improved their tolerance to Verticillium wilt (Figures 5 and S6). And the expression level of SA-dependent and JA-dependent defence pathway-related genes were significantly increased in VP2 over-expressing transgenic cotton, and the SA and JA contents were also significantly increased (Figure 6). In conclusion, our results illustrate that VP2 expression confers resistance to *V. dahliae* in cotton through the activation of defence responses without affecting the growth and development of transgenic cotton.

Experimental procedures

Pathogen infection and disease assay

V. dahliae cultivation was performed as described previously (Xu *et al*., 2011). *V. dahliae* was inoculated on a potato dextrose agar (PDA) plate for 4 days and placed in an incubator at 25 °C. Fungal colonies were transferred into Czapek medium on a shaker at 120 rpm at 25 °C for 4 days. Three-week-old cotton seedlings were inoculated by the root-dip method. The disease index was scored using at least 30 plants per treatment and repeated at least three times. The plant disease index was calculated according to previously described methods (Xu *et al*., 2011). Experiments were maintained at a constant temperature of 25 °C to 28 °C under long-day conditions with an 8-h/16-h dark/light photoperiod and a relative humidity of 60%.

Fungus sample preparation and RNA-seq

G. barbadense cv. 7124 and *G. hirsutum* cv. YZ1 were grown in sterile seedling culture medium for about 7 days. The roots were cut into about 1 cm segments and put into either V991 and 1cd3-2 culture medium and cultured on a shaker at 25 °C and 150 rpm for 3 days. After 3 days, the roots were filtered on gauze and then put it into a centrifuge tube at 5000 rpm for 15 min to remove the supernatant, and the precipitation of V991 or 1cd3-2 was used for RNA extraction and transcriptome sequencing, respectively. V991 and 1cd3-2 without cotton root treatment were used as control.

The RNA extraction of *V. dahliae* was carried out according to the instructions of the fungus RNA extraction kit (OMEGA, R6840-02). The library preparations were sequenced on an Illumina Novaseq6000 platform and 150 bp single reads were generated. RNA-Seq reads were aligned to V991 or 1cd3-2 genomes (unpublished), respectively, using Hisat2 with default parameters. Transcripts of each sample were assembled using Stringtie (Pertea *et al*., 2016). edgeR package was used to find the expression differences between samples.

Secretome analysis

To perform secretome analysis, V991 was pre-cultured on PDA media for 4 days and placed in an incubator at 25 °C and transferred to liquid Czapek medium on a shaker at 120 rpm at 25 °C. Sterile cotton roots were added in the treatment group, but not in the control group. Three days later, the culture medium was filtered, centrifuged, and the supernatant was filtered on a 0.22 μm filter membrane to remove the mycelium and other impurities, and then centrifuged in 3 KD ultrafiltration centrifuge tubes. Finally, the secreted protein of *V. dahliae* was identified by using label-free technology (Cox *et al*., 2014). In the analysis of significance difference of quantitative results, at least two non-null values of three repeated experimental data in the selected sample group were statistically analysed, and the differentially expressed proteins were identified using the following filter criteria: $P \leq 0.05$ and fold change ≥2.

Expression pattern analysis

Quantitative real-time PCR (qRT-PCR) was performed using a 7500 real time PCR system (ABI, Foster City, CA) with the iTag™ Universal SYBR Green Supermix (Bio-Rad, Hercules, CA) in a 15 μL reaction volume. qRT-PCR was performed as follows: an initial 95 °C denaturation step for 3 min, followed by 40 cycles of 95 °C for 15 s and 60 °C for 45 s. The house-keeping genes *GhUB7*, *NbEF1a*, and *v991_EVM0005718* were used as internal controls for cotton, *N. benthamiana* and *V. dahliae*, respectively. Primers used in this study are listed in Table S2.

Prokaryotic expression protein

The target gene was constructed in the GST label vector pGEX-4T-1 through the BP and LR reactions of Gateway cloning system, and the constructed label vector was introduced into the prokaryotic expression strain BL21. The monoclone was selected and then shaken in medium in a triangular flask. IPTG (0.5 M) was added when the OD600 was 0.6–0.8, and the expression was induced at 16 °C for 12–16 h. The cells were lysed followed by sonication, and 1 mM protein supernatant of prokaryotic expression was used for injection into cotton cotyledons. The cotton plantlets were kept under greenhouse conditions of 25 °C to 28 °C under long days with an 8-h/16-h dark/light photoperiod and a relative humidity of 60%.

Analysis of subcellular localization

The *V. dahliae* candidate effector v991_EVM0004415 (VP2) was amplified from a V991 cDNA library with specific primers (Table S2). The variants VP2^{-sp} (without SP) and VP2(1cd3-2) (with the signal peptide of VP2 fused into VP2^{-sp}) were cloned into vector pGWB743. The GFP was used as a control. CBLn, which localizes to the plant plasma membrane, was used as a positive control in localization studies. Three vectors were separately introduced into *A. tumefaciens* strain GV3101, and *N. benthamiana* leaves were infiltrated with the bacterial suspension (OD600 = 0.5–0.8). Two days post-agroinfiltration, the infiltrated leaves were cut to observe GFP and RFP fluorescence of using confocal microscopy (Olympus FV1200). Primers used in this study are listed in Table S2.

VIGS in *N. benthamiana*

The vectors pTRV1 and pTRV2 were used for the VIGS assay (Gao *et al*., 2013). Genes sequences of *NbBAK1*, *NbSOBIR1*, *GFP*, and *PDS* were inserted into pTRV2. The primer sequences are listed in Table S2. All vectors were separately introduced into *A. tumefaciens* strain GV3101. All *Agrobacterium* cultures containing pTRV1 and pTRV2-genes were adjusted to OD600 = 0.5–0.8. pTRV2-GFP was used as a control, and pTRV2-PDS was used to evaluate the efficiency of VIGS. RNA extracted from *N. benthamiana* leaves was used to verify the efficiency of gene silencing by qRT-PCR.

Yeast signal sequence trap system

Functional validation of the predicted signal peptide was performed as described previously (Ma *et al*., 2021). In brief, the predicted signal peptide (SP) was cloned into pSUC2, and the resulting plasmid was transformed into YTK12, an invertase mutant yeast strain. The positive transformants were incubated on YPRAA medium (2% raffinose). Invertase enzymatic activity was assayed by 2,3,5-triphenyltetrazolium chloride reduction assay (Schenke *et al*., 2011). The empty pSUC2 and pSUC2-Avr1bSP vectors were used as negative and positive controls, respectively.

Generation of gene deletion mutants and mutant complementation

Generation of targeted gene deletion constructs was based on the previously described method (Zhang *et al*., 2017). In order to produce complementary transformants, VP2 was cloned into the binary vector p823-GFP carrying resistance to G418, and VP2 was reintroduced to the *ΔVP2* strains. Complemented transformants were obtained using a previously described Agrobacterium-mediated transformation method (Zhang *et al*., 2017). All primers used are listed in Table S2.

Plant transformation, protein extraction, and western blotting

VP2 was amplified and inserted into the 4 × MYC label vector pPGWB417 through the BP and LR reactions of Gateway cloning system to generate the overexpression vector. The VP2 over-expressing vector was introduced into *Agrobacterium tumefaciens* (strain GV3101) and used to transform cotton according to previous methods (Li *et al*., 2019). The primers used in this study are listed in Table S2.

To perform western blotting, firstly sampled leaves were ground into fine powder using liquid nitrogen, and then 0.1 g of sample was put into a 2 mL centrifuge tube. 200 μL of protein lysate (P0013, Biyuntian) (1% protease inhibitor has been added) was added, shaken and mixed quickly, and then incubated on ice for 40 min. The mixture was centrifuged at 4 °C for 15 min at 12 000 rpm, and supernatant was taken for SDS-PAGE electrophoresis.

Sample preparation and RNA-seq of VP2 expressing transgenic cotton

RNA from wild-type and VP2 overexpressing cotton was extracted for transcriptome sequencing before and at 12 h post inoculation

with V991. Total RNA was extracted using an RNA Extraction Kit (Tiangen Biotech, Beijing, China). The library preparations were sequenced on an Illumina Novaseq6000 platform, and 150 bp paired-end reads were generated. Sequencing adapters were removed and consecutive low-quality bases were trimmed from both the 5′ and 3′ end of the reads, high-quality RNA-Seq reads were aligned to the cotton genome (Wang *et al*., 2019), using Hisat2 with default parameters. Transcripts of each sample were assembled using Stringtie (Pertea *et al*., 2016). edgeR package was used to find the expression differences between samples.

Measurement of phytohormones

The roots of cotton plantlets at the same growing stage were taken and quickly ground into powder using liquid nitrogen, then 0.1 g of samples were placed into a 2 mL centrifuge tube, then homogenized in 700 μL 80% (v/v) methanol and shaken overnight at 4 °C in the dark. Samples were then centrifuged for 15 min at 12 000 rpm and 4 °C, the supernatant was collected, and 300 μL precooled extraction buffer was added to the sediment. After 1 h of oscillation extraction at 4 °C, centrifugation was performed at 4 °C and 12 000 rpm for 15 min, supernatant was collected twice and combined, then filtered through 0.22 μm filter membrane (JINTENG Biotech, Tianjin, China). HPLC-MS/MS (AB SCIEX Triple Quad 5500 LC/MS/MS system) was used to measure plant hormones, and internal standard settings were according to previous studies (Sun *et al*., 2014).

Histochemical staining and determination of lignin content

Lignin deposition in plant hypocotyls was measured according to previously described method (Xu *et al*., 2011). In brief, sample sections of cotton plants were dipped in phloroglucinol solution (3% w/v phloroglucinol in 95% ethanol) for 10 min, then transferred to 18% HCl for 5 min, and photographed under a Leica fluorescence microscope (DM2500, Leica, Germany). The lignin content of roots was determined using the method as described previously by Xu *et al*. (2011).

Acknowledgements

Designed Project: L.F.Z., X.L.Z; Material Preparation: P.Q.; Experiments: P.Q., B.X.Z., H.Y., Z.G.Y., Y.W., Y.Q.M.; Field test: J.K.; Visualization: P.Q.; Writing Manuscripts: P.Q.; Revising manuscripts: L.F.Z., K.L., M.S., L.Z., Q.H, X.L.Z. All authors read and approved the paper. This work was supported by the fundings from The Ministry of Agriculture and Rural Affairs of China (2022YFD1200303) and Hubei Hongshan Laboratory (2022hszd004).

Conflict of interest

The authors declared that no conflicts of interest exist.

Data availability

The raw RNA-seq data generated in this paper have been deposited in the Genome Sequence Archive (Genomics, Proteomics & Bioinformatics 2021) in National Genomics Data Center (Nucleic Acids Res 2022), China National Center for Bioinformation / Beijing Institute of Genomics, Chinese Academy of Sciences (GSA: CRA011235 and CRA011237) that are publicly accessible. All supporting data from this study are available from the article and supplementary information files, or from the corresponding author upon reasonable request.

References

Asai, S., Furzer, O.J., Cevik, V., Kim, D.S., Ishaque, N., Goritschnig, S., Staskawicz, B.J. *et al*. (2018) A downy mildew effector evades recognition by polymorphism of expression and subcellular localization. *Nat. Commun.* **9**, 5192.

Bi, K., Liang, Y., Mengiste, T. and Sharon, A. (2023) Killing softly: a roadmap of *Botrytis cinerea* pathogenicity. *Trends Plant Sci.* **28**, 211–222.

Cao, Y., Liang, Y., Tanaka, K., Nguyen, C.T., Jedrzejczak, R.P., Joachimiak, A. and Stacey, G. (2014) The kinase LYK5 is a major chitin receptor in Arabidopsis and forms a chitin-induced complex with related kinase CERK1. *Elife*, **3**, e03766.

Castroverde, C.D.M., Nazar, R.N. and Robb, J. (2016) Verticillium Ave1 effector induces tomato defense gene expression independent of Ve1 protein. *Plant Signal. Behav.* **11**, e1245254.

Chen, J.Y., Liu, C., Gui, Y.J., Si, K.W., Zhang, D.D., Wang, J., Short, D.P.G. *et al*. (2018) Comparative genomics reveals cotton-specific virulence factors in flexible genomic regions in *Verticillium dahliae* and evidence of horizontal gene transfer from Fusarium. *New Phytol.* **217**, 756–770.

Chinchilla, D., Zipfel, C., Robatzek, S., Kemmerling, B., Nurnberger, T., Jones, J.D., Felix, G. *et al*. (2007) A flagellin-induced complex of the receptor FLS2 and BAK1 initiates plant defence. *Nature*, **448**, 497–500.

Chinchilla, D., Shan, L., He, P., de Vries, S. and Kemmerling, B. (2009) One for all: the receptor-associated kinase BAK1. *Trends Plant Sci.* **14**, 535–541.

Cox, J., Hein, M.Y., Luber, C.A., Paron, I., Nagaraj, N. and Mann, M. (2014) Accurate proteome-wide label-free quantification by delayed normalization and maximal peptide ratio extraction, termed MaxLFQ. *Mol. Cell. Proteomics*, **13**, 2513–2526.

Du, Q., Yang, X., Zhang, J., Zhong, X., Kim, K.S., Yang, J., Xing, G. *et al*. (2018) Over-expression of the *Pseudomonas syringae* harpin-encoding gene hrpZm confers enhanced tolerance to Phytophthora root and stem rot in transgenic soybean. *Transgenic Res.* **27**, 277–288.

Escocard de Azevedo Manhães, A.M., Ortiz-Morea, F.A., He, P. and Shan, L. (2021) Plant plasma membrane-resident receptors: Surveillance for infections and coordination for growth and development. *J. Integr. Plant Biol.* **63**, 79–101.

Fradin, E.F. and Thomma, B.P. (2006) Physiology and molecular aspects of Verticillium wilt diseases caused by *V. dahliae* and *V. albo-atrum*. *Mol. Plant Pathol.* **7**, 71–86.

Fu, M., Xu, M., Zhou, T., Wang, D., Tian, S., Han, L., Dong, H. *et al*. (2014) Transgenic expression of a functional fragment of harpin protein Hpa1 in wheat induces the phloem-based defence against *English grain aphid*. *J. Exp. Bot.* **65**, 1439–1453.

Gao, W., Long, L., Zhu, L.F., Xu, L., Gao, W.H., Sun, L.Q., Liu, L.L. *et al*. (2013) Proteomic and virus-induced gene silencing (VIGS) analyses reveal that gossypol, brassinosteroids, and jasmonic acid contribute to the resistance of cotton to *Verticillium dahliae*. *Mol. Cell. Proteomics*, **12**, 3690–3703.

Glazebrook, J., Chen, W., Estes, B., Chang, H.S., Nawrath, C., Métraux, J.P., Zhu, T. *et al*. (2003) Topology of the network integrating salicylate and jasmonate signal transduction derived from global expression phenotyping. *Plant J.* **34**, 217–228.

Guttman, D.S., McHardy, A.C. and Schulze-Lefert, P. (2014) Microbial genome-enabled insights into plant-microorganism interactions. *Nat. Rev. Genet.* **15**, 797–813.

He, F., Wang, C., Sun, H., Tian, S., Zhao, G., Liu, C., Wan, C. *et al*. (2023) Simultaneous editing of three homoeologues of TaCIPK14 confers broad-spectrum resistance to stripe rust in wheat. *Plant Biotechnol. J.* **21**, 354–368.

Hu, Q., Zhu, L., Zhang, X., Guan, Q., Xiao, S., Min, L. and Zhang, X. (2018) GhCPK33 negatively regulates defense against *Verticillium dahliae* by phosphorylating GhOPR3. *Plant Physiol.* **178**, 876–889.

Huang, J., Chen, L., Lu, X., Peng, Q., Zhang, Y., Yang, J., Zhang, B.Y. *et al*. (2018) Natural allelic variations provide insights into host adaptation of *Phytophthora* avirulence effector PsAvr3c. *New Phytol.* **221**, 1010–1022.

Inderbitzin, P. and Subbarao, K.V. (2014) Verticillium systematics and evolution: how confusion impedes Verticillium wilt management and how to resolve it. *Phytopathology*, **104**, 564–574.

Jiménez-Díaz, R.M., Olivares-García, C., Landa, B.B., del Mar Jiménez-Gasco, M. and Navas-Cortés, J.A. (2011) Region-wide analysis of genetic diversity in *Verticillium dahliae* populations infecting olive in southern Spain and agricultural factors influencing the distribution and prevalence of vegetative compatibility groups and pathotypes. *Phytopathology*, **101**, 304–315.

John, E., Jacques, S., Phan, H.T.T., Liu, L., Pereira, D., Croll, D., Singh, K.B. *et al*. (2022) Variability in an effector gene promoter of a necrotrophic fungal pathogen dictates epistasis and effector-triggered susceptibility in wheat. *PLoS Pathog.* **18**, e1010149.

Jones, J. and Dangl, J.L. (2006) The plant immune system. *Nature*, **444**, 323–329.

Jonge, R.D., Bolton, M., Kombrink, A., Van, D., Yadeta, K.A. and Thomma, B. (2013) Extensive chromosomal reshuffling drives evolution of virulence in an asexual pathogen. *Genome Res.* **23**, 1271–1282.

Lai, M., Cheng, Z., Xiao, L., Klosterman, S.J. and Wang, Y. (2022) The bZip transcription factor VdMRTF1 is a negative regulator of melanin biosynthesis and virulence in *Verticillium dahliae*. *Microbiol. Spectr.* **10**, e0258121.

Li, L., Kim, P., Yu, L., Cai, G., Chen, S., Alfano, J.R. and Zhou, J.M. (2016) Activation-dependent destruction of a co-receptor by a *Pseudomonas syringae* effector dampens plant immunity. *Cell Host Microbe.* **20**, 504–514.

Li, J., Wang, M., Li, Y., Zhang, Q., Lindsey, K., Daniell, H., Jin, S. *et al*. (2019) Multi-omics analyses reveal epigenomics basis for cotton somatic embryogenesis through successive regeneration acclimation process. *Plant Biotechnol. J.* **17**, 435–450.

Li, Z., Zhang, Y., Ren, J., Jia, F., Zeng, H., Li, G. and Yang, X. (2022) Ethylene-responsive factor ERF114 mediates fungal pathogen effector PevD1-induced disease resistance in *Arabidopsis thaliana*. *Mol. Plant Pathol.* **23**, 819–831.

Li, X., Niu, G., Fan, Y., Liu, W., Wu, Q., Yu, C., Wang, J. *et al*. (2023) Synthetic dual hormone-responsive promoters enable engineering of plants with broad-spectrum resistance. *Plant Commun.* **4**, 100596.

Liang, Y., Li, Z., Zhang, Y., Meng, F., Qiu, D., Zeng, H., Li, G. *et al*. (2021) Nbnrp1 mediates *Verticillium dahliae* effector PevD1-triggered defense responses by regulating sesquiterpenoid phytoalexins biosynthesis pathway in *Nicotiana benthamiana*. *Gene*, **768**, 145280.

Ma, Z., Song, T., Zhu, L., Ye, W., Wang, Y., Shao, Y., Dong, S. *et al*. (2015) A *Phytophthora sojae* glycoside hydrolase 12 protein is a major virulence factor during soybean infection and is recognized as a PAMP. *Plant Cell*, **27**, 2057–2072.

Ma, A., Zhang, D., Wang, G., Wang, K., Li, Z., Gao, Y., Li, H. *et al*. (2021) *Verticillium dahliae* effector VDAL protects MYB6 from degradation by interacting with PUB25 and PUB26 E3 ligases to enhance Verticillium wilt resistance. *Plant Cell*, **33**, 3675–3699.

Miao, W., Wang, X., Li, M., Song, C., Wang, Y., Hu, D. and Wang, J. (2010) Genetic transformation of cotton with a harpin-encoding gene hpaXoo confers an enhanced defense response against different pathogens through a priming mechanism. *BMC Plant Biol.* **10**, 67.

Ngou, B.P.M., Ahn, H.K., Ding, P. and Jones, J.D.G. (2021) Mutual potentiation of plant immunity by cell-surface and intracellular receptors. *Nature*, **592**, 110–115.

Nomoto, M., Skelly, M.J., Itaya, T., Mori, T., Suzuki, T., Matsushita, T., Tokizawa, M. *et al*. (2021) Suppression of MYC transcription activators by the immune cofactor NPR1 fine-tunes plant immune responses. *Cell Rep.* **37**, 110125.

Okmen, B., Jaeger, E., Schilling, L., Finke, N., Klemd, A., Lee, Y.J., Wemhoner, R. *et al*. (2022) A conserved enzyme of smut fungi facilitates cell-to-cell extension in the plant bundle sheath. *Nat. Commun.* **13**, 6003.

Pemberton, C.L. and Salmond, G.P. (2004) The Nep1-like proteins-a growing family of microbial elicitors of plant necrosis. *Mol. Plant Pathol.* **5**, 353–359.

Pertea, M., Kim, D., Pertea, G.M., Leek, J.T. and Salzberg, S.L. (2016) Transcript-level expression analysis of RNA-seq experiments with HISAT, StringTie and Ballgown. *Nat. Protoc.* **11**, 1650–1667.

Qin, J., Wang, K., Sun, L., Xing, H., Wang, S., Li, L., Chen, S. *et al*. (2018) The plant-specific transcription factors CBP60g and SARD1 are targeted by a Verticillium secretory protein VdSCP41 to modulate immunity. *eLife*, **7**, e34902.

Rajput, N.A., Zhang, M., Shen, D., Liu, T., Zhang, Q., Ru, Y., Sun, P. *et al*. (2015) Overexpression of a phytophthora cytoplasmic CRN effector confers resistance to disease, salinity and drought in *Nicotiana benthamiana*. *Plant Cell Physiol.* **56**, 2423–2435.

Sands, L.B., Cheek, T., Reynolds, J., Ma, Y. and Berkowitz, G.A. (2022) Effects of harpin and Flg22 on growth enhancement and pathogen defense in cannabis sativa seedlings. *Plants (Basel)*, **11**, 1178.

Schenke, D., Bottcher, C. and Scheel, D. (2011) Crosstalk between abiotic ultraviolet-B stress and biotic (flg22) stress signalling in Arabidopsis prevents flavonol accumulation in favor of pathogen defence compound production. *Plant Cell Environ.* **34**, 1849–1864.

Song, T., Zhang, Y., Zhang, Q., Zhang, X., Shen, D., Yu, J., Yu, M. *et al*. (2021) The N-terminus of an *Ustilaginoidea virens* Ser-Thr-rich glycosylphosphatidylinositol-anchored protein elicits plant immunity as a MAMP. *Nat. Commun.* **12**, 2451.

Sun, Y., Li, L., Macho, A.P., Han, Z., Hu, Z., Zipfel, C., Zhou, J.M. *et al*. (2013) Structural basis for flg22-induced activation of the Arabidopsis FLS2-BAK1 immune complex. *Science*, **342**, 624–628.

Sun, L., Zhu, L., Xu, L., Yuan, D., Min, L. and Zhang, X. (2014) Cotton cytochrome P450 CYP82D regulates systemic cell death by modulating the octadecanoid pathway. *Nat. Commun.* **5**, 5372.

Tao, Z., Liu, H., Qiu, D., Zhou, Y., Li, X., Xu, C. and Wang, S. (2009) A pair of allelic WRKY genes play opposite roles in rice-bacteria interactions. *Plant Physiol.* **151**, 936–948.

Tian, B., Xie, J., Fu, Y., Cheng, J., Li, B., Chen, T., Zhao, Y. *et al*. (2020) A cosmopolitan fungal pathogen of dicots adopts an endophytic lifestyle on cereal crops and protects them from major fungal diseases. *ISME J.* **14**, 3120–3135.

Wang, M., Tu, L., Yuan, D., Zhu, D., Shen, C., Li, J., Liu, F. *et al*. (2019) Reference genome sequences of two cultivated allotetraploid cottons, *Gossypium hirsutum* and *Gossypium barbadense*. *Nat. Genet.* **51**, 224–229.

Wang, W., Feng, B., Zhou, J.M. and Tang, D. (2020) Plant immune signaling: Advancing on two frontiers. *J. Integr. Plant Biol.* **62**, 2–24.

Wang, D., Chen, J.Y., Song, J., Li, J.J., Klosterman, S.J., Li, R., Kong, Z.Q. *et al*. (2021) Cytotoxic function of xylanase VdXyn4 in the plant vascular wilt pathogen *Verticillium dahliae*. *Plant Physiol.* **187**, 409–429.

Wang, D., Zhang, D.D., Song, J., Li, J.J., Wang, J., Li, R., Klosterman, S.J. *et al*. (2022a) *Verticillium dahliae* CFEM proteins manipulate host immunity and differentially contribute to virulence. *BMC Biol.* **20**, 55.

Wang, L., Liu, H., Zhang, M., Ye, Y., Wang, L., Zhu, J., Chen, Z. *et al*. (2022b) Microbe-derived non-necrotic glycoside hydrolase family 12 proteins act as immunogenic signatures triggering plant defenses. *J. Integr. Plant Biol.* **64**, 1966–1978.

van Wees, S.C., de Swart, E.A., van Pelt, J.A., van Loon, L.C. and Pieterse, C.M. (2000) Enhancement of induced disease resistance by simultaneous activation of salicylate- and jasmonate-dependent defense pathways in *Arabidopsis thaliana*. *Proc. Natl. Acad. Sci. U. S. A.* **97**, 8711–8716.

Wittkopp, P.J., Haerum, B.K. and Clark, A.G. (2004) Evolutionary changes in cis and trans gene regulation. *Nature*, **430**, 85–88.

Woolhouse, M.E., Webster, J.P., Domingo, E., Charlesworth, B. and Levin, B.R. (2002) Biological and biomedical implications of the co-evolution of pathogens and their hosts. *Nat. Genet.* **32**, 569–577.

Xiang, Y., Song, M., Wei, Z., Tong, J., Zhang, L., Xiao, L., Ma, Z. *et al*. (2011) A jacalin-related lectin-like gene in wheat is a component of the plant defence system. *J. Exp. Bot.* **62**, 5471–5483.

Xiao, S., Hu, Q., Zhang, X., Si, H., Liu, S., Chen, L., Chen, K. *et al*. (2021) Orchestration of plant development and defense by indirect crosstalk of salicylic acid and brassinosteorid signaling via transcription factor GhTINY2. *J. Exp. Bot.* **72**, 4721–4743.

Xie, T., Wu, X., Luo, L., Qu, Y., Fan, R., Wu, S., Long, Y. *et al*. (2023) Natural variation in the hrpL promoter renders the phytopathogen *Pseudomonas syringae* pv. actinidiae nonpathogenic. *Mol. Plant Pathol.* **24**, 262–271.

Xu, L., Zhu, L., Tu, L., Liu, L., Yuan, D., Jin, L., Long, L. *et al*. (2011) Lignin metabolism has a central role in the resistance of cotton to the wilt fungus *Verticillium dahliae* as revealed by RNA-Seq-dependent transcriptional analysis and histochemistry. *J. Exp. Bot.* **62**, 5607–5621.

Xu, G., Yuan, M., Ai, C., Liu, L., Zhuang, E., Karapetyan, S., Wang, S. *et al*. (2017) uORF-mediated translation allows engineered plant disease resistance without fitness costs. *Nature*, **545**, 491–494.

Yu, C., Dou, K., Wang, S., Wu, Q., Ni, M., Zhang, T., Lu, Z. *et al*. (2020) Elicitor hydrophobin Hyd1 interacts with Ubiquilin1-like to induce maize systemic resistance. *J. Integr. Plant Biol.* **62**, 509–526.

Yuan, M., Jiang, Z., Bi, G., Nomura, K., Liu, M., Wang, Y., Cai, B. *et al*. (2021) Pattern-recognition receptors are required for NLR-mediated plant immunity. *Nature*, **592**, 105–109.

Zhang, L., Ni, H., Du, X., Wang, S., Ma, X.-W., Nürnberger, T., Guo, H.-S. *et al*. (2017) The Verticillium-specific protein VdSCP7 localizes to the plant nucleus and modulates immunity to fungal infections. *New Phytol.* **215**, 368–381.

Zhang, L., Yan, J., Fu, Z., Shi, W., Ninkuu, V., Li, G., Yang, X. *et al*. (2021) FoEG1, a secreted glycoside hydrolase family 12 protein from *Fusarium oxysporum*, triggers cell death and modulates plant immunity. *Mol. Plant Pathol.* **22**, 522–538.

Zhang, Y., Yin, Z., Pi, L., Wang, N., Wang, J., Peng, H. and Dou, D. (2023) A *Nicotiana benthamiana* receptor-like kinase regulates *Phytophthora* resistance by coupling with BAK1 to enhance elicitin-triggered immunity. *J. Integr. Plant Biol.* **65**, 1553–1565.

Zhou, J.M. and Zhang, Y. (2020) Plant immunity: Danger perception and signaling. *Cell*, **181**, 978–989.

Zhu, D., Zhang, X., Zhou, J., Wu, Y., Zhang, X., Feng, Z., Wei, F. *et al*. (2021) Genome-wide analysis of ribosomal protein GhRPS6 and its role in cotton Verticillium wilt resistance. *Int. J. Mol. Sci.* **22**, 1795.

Zuo, N., Bai, W.Z., Wei, W.Q., Yuan, T.L., Zhang, D., Wang, Y.Z. and Tang, W.H. (2022) Fungal CFEM effectors negatively regulate a maize wall-associated kinase by interacting with its alternatively spliced variant to dampen resistance. *Cell Rep.* **41**, 111877.

Supporting information

Additional supporting information may be found online in the Supporting Information section at the end of the article.

Figure S1 Lable-free-based secretome of V991. (a) Principle component analysis of 790 proteins detected in all samples. (b) Venn diagram to show the number of proteins identified in the control group and the treatment group. (c) and (d) Statistics of amino acid length (c) and cysteine number (d) of 286 secreted proteins (possess the extracellular localization signal peptide and lack a transmembrane motif).

Figure S2 Expression profiling of candidate secretory proteins (VPs) in V991 and 1cd3-2 transcriptomes, respectively.

Figure S3 The amino acid sequence alignment of the D-type VP2 (genotype of VP2 in the V991 genome) and ND-type VP2 (genotype of VP2 in the 1cd3-2 genome). Numbers represent the position of the amino acid (aa) residues, and sequence alignments were performed with ClustalX 2.1.

Figure S4 The signal peptide (SP) of D-type VP2 and ND-type VP2 are functional. YPRAA medium for verification of secretion activity on invertase. TTC assay for the test of secreted invertase activity. Note that only the strain expressing the Avr1b, D-type VP2, and ND-type VP2 SP fusion gained the ability to catabolize raffinose and reduce 2, 3, 5-triphenyltetrazolium chloride (TTC) into red formazan. Both YPRAA and TTC indicate the successful secretion of the invertase.

Figure S5 The growth rate and mycelium morphology of the wild-type V991, *ΔVP2* mutant, and *ΔVP2*/VP2-complementation transformants. (a) PCR analysis of wild-type strain V991 and *ΔVP2* mutants. The genomic DNA of each strain was used to verify the 5′ and 3′ homologous and presence of targeted gene. (b) Growth rate assay of the wild-type V991, *ΔVP2* mutant, and *ΔVP2*/VP2-complementation transformants. Each assay was replicated three times. No significant differences compared with the WT were found (Student's *t* test). (c) Mycelium morphology of the wild-type V991, *ΔVP2* mutant, and *ΔVP2*/VP2-complementation transformants. Images of wild-type V991, *ΔVP2* mutant, and *ΔVP2*/VP2-complementation transformants cultured on PDA plates at 25 °C for 7 days in the dark. Scale bars, 100 μm. Each assay was replicated three times.

Figure S6 *OEVP2* plants enhanced resistance to *V. dahliae* in the field. (a) The photos for the two transgenic lines (*OEVP2-1* and *OEVP2-2*) and wild-type plants growing in the same field infected with *V. dahliae*. Scale bars, 10 cm. (b) The statistics of disease grade in the field condition, count with at least 20 plants. Statistical analyses were performed using a Student's *t* test: $*P < 0.05$; $**P < 0.01$.

Figure S7 qRT-PCR analysis of other lignin synthesis related genes in VP2 transgenic cotton lines without inoculation. The values are means ± SD, $n = 3$, and normalized with *GhUB7*, and then all values in *WT* were normalized as 1. Statistical analyses were performed using a Student's *t* test: ns, Not significant; $*P < 0.05$; $***P < 0.001$.

Table S1 Identified *Verticillium dahliae* secreted proteins.

Table S2 Primers used in the study.

Table S3 Common proteins identified in the control and treatment groups of secretome.

Table S4 Specific proteins identified in the control or treatment group of secretome.